

# On Fermi acceleration and MHD-instabilities at ultra-relativistic magnetized shock waves

Guy Pelletier<sup>1\*</sup>, Martin Lemoine<sup>2†</sup> and Alexandre Marcowith<sup>3‡</sup>

<sup>1</sup> *Laboratoire d'Astrophysique de Grenoble,*

*CNRS, Université Joseph Fourier II, BP 53, F-38041 Grenoble, France;*

<sup>2</sup> *Institut d'Astrophysique de Paris,*

*UMR 7095 CNRS, Université Pierre & Marie Curie, 98 bis boulevard Arago, F-75014 Paris, France*

<sup>3</sup> *Laboratoire de Physique Théorique et Astroparticules,*

*CNRS, Université Montpellier-II, place Eugène Bataillon, 34095 Montpellier Cédex, France*

## ABSTRACT

Fermi acceleration can take place at ultra-relativistic shock waves if the upstream or downstream magnetic field has been remodeled so that most of the magnetic power lies on short spatial scales. The relevant conditions under which Fermi acceleration become efficient in the presence of both a coherent and a short scale turbulent magnetic field are addressed. Within the MHD approximation, this paper then studies the amplification of a pre-existing magnetic field through the streaming of cosmic rays upstream of a relativistic shock wave. The magnetic field is assumed to be perpendicular in the shock front frame, as generally expected in the limit of large shock Lorentz factor. In the MHD regime, compressive instabilities seeded by the net cosmic-ray charge in the shock precursor (as seen in the shock front frame) develop on the shortest spatial scales but saturate at a moderate level  $\delta B/B \sim 1$ , which is not sufficient for Fermi acceleration. As we argue, it is possible that other instabilities outside the MHD range provide enough amplification to allow successful Fermi acceleration.

**Key words:** shock waves – acceleration of particles – cosmic rays

## 1 INTRODUCTION

The physics of collisionless shock waves is of paramount importance in modern astrophysics, as it governs a variety of phenomena, most notably the emission of high energy radiation. In particular, the afterglow radiation of gamma-ray bursts is generally attributed to the synchrotron emission of electrons that have been accelerated around the relativistic external shock wave, with shock Lorentz factor  $\Gamma_{\text{sh}} \sim 100$  (Paczynski & Rhoads 1993, Katz 1994, Mészáros & Rees 1997, Sari & Piran 1997, Vietri 1997, Waxman 1997; see Piran 2005 for a review). In this framework, it can be shown that the magnetic field, downstream of the shock wave, must have been amplified by orders of magnitude beyond the shock compression of a typical interstellar magnetic field (see for instance Waxman 1997; see also Piran 2005 and references therein). Recent work by Li & Waxman (2006) further shows that even the upstream magnetic field must have been amplified by at least one or two orders of magnitude in order to explain observed X-ray afterglows.

These results should be put in perspective with recent studies on the process of Fermi acceleration in the test particle limit around relativistic shock waves. In particular, Niemiec & Ostrowski (2006)

have shown that Fermi acceleration becomes inoperative in a turbulent magnetic field with power spectra of the Kolmogorov or scale invariant type. Through analytical calculations, Lemoine, Pelletier & Revenu (2006) have shown that relativistic Fermi acceleration is inefficient if the magnetic field power is distributed on scales larger than the typical Larmor radius of the accelerated population, in agreement with the above numerical result. Therefore the interpretation of the gamma-ray burst afterglow emission from the relativistic external shock wave requires the magnetic field to have been amplified on short spatial scales.

It has been suggested that the relativistic two stream Weibel instability could amplify the downstream magnetic field to the level required by afterglow modeling of gamma-ray bursts (Gruzinov & Waxman 1999; Medvedev & Loeb 1999). Subsequent studies have however argued that this instability should saturate early on (Wiersma & Achterberg 2004; Lyubarsky & Eichler 2006). The question of the long term evolution of the downstream magnetic field (on timescales  $\gg \omega_p^{-1}$ , with  $\omega_p$  the plasma frequency) also remains open. Ongoing particle-in-cell simulations should eventually shed light on this issue (Silva *et al.* 2003; Frederiksen *et al.* 2004; Medvedev *et al.* 2005; Kato 2007; Chang, Spitkovsky & Arons 2008; Keshet *et al.* 2008; Spitkovsky 2008).

Regarding the amplification of the upstream magnetic field, the present situation is reminiscent of results obtained for non-relativistic supernovae remnant shock waves, where the interstellar

\* e-mail: [guy.pelletier@obs.ujf-grenoble.fr](mailto:guy.pelletier@obs.ujf-grenoble.fr)

† e-mail: [lemoine@iap.fr](mailto:lemoine@iap.fr)

‡ e-mail: [alexandre.marcowith@lpta.in2p3.fr](mailto:alexandre.marcowith@lpta.in2p3.fr)

magnetic field has apparently been amplified by one or two orders of magnitude (see Völk, Berezhko & Ksenofontov 2005, Parizot *et al.* 2006). In this case, the leading candidate for the instability is the streaming instability, seeded by the cosmic ray precursor in the upstream plasma (see Bell 2004, 2005; Pelletier, Lemoine & Marcowith 2006, Marcowith, Lemoine & Pelletier 2006; Reville *et al.* 2007; Niemiec *et al.* 2008; Amato & Blasi 2008; Zirakashvili, Ptuskin & Völk 2008; Reville *et al.* 2008). The generalization of this instability to the relativistic regime has been studied on phenomenological grounds by Milosavljević & Nakar (2006) who have concluded that it should be able to account for the degree of amplification inferred in gamma-ray bursts. More recently, Reville, Kirk & Duffy (2006) have derived in detail the dispersion relation for a parallel shock wave and the saturation due to thermal effects.

In the present work, we propose to explore in detail the generalization of this type of instability to the ultra-relativistic regime  $\Gamma_{\text{sh}} \gg 1$ . One crucial difference with the previous works on the streaming instability is that we consider the most natural case of superluminal shock waves (with a magnetic field perpendicular to the shock normal in the shock front frame). This case is more generic than the parallel configuration studied previously because the transverse component of the magnetic field is boosted by the shock Lorentz factor when going to the shock frame. Another important difference is that we bring to light a new type of instability, of a compressive nature. Finally, in contrast with most particle-in-cell simulations performed to date, our study focusses on magnetized shock waves, for which there exists a coherent upstream magnetic field (whose dynamical influence on the shock jump conditions can be neglected however). Nevertheless there exist pioneering PIC simulations in the moderately relativistic regime, which include both a mean field and a significant mass ratio between electrons and ions, see Hededal & Nishikawa (2005), Dieckmann, Shukla, & Drury (2008).

We adopt a simplified description in which the cosmic-ray distribution is modeled as a step function out to some distance  $\ell_{\text{cr}}$  and we neglect the cosmic-ray response to the disturbance. This latter assumption is justified by the fact that the instability is maximal on the shortest spatial scales, orders of magnitude below the typical Larmor radius of accelerated particles.

The paper is organized as follows. In Section 2, we introduce the main scales of the problem, most notably the diffusion scale of the cosmic rays; we then calculate the level of amplification that is necessary to make Fermi acceleration operative. Section 3 is devoted to the investigation of the instabilities under the condition that some cosmic-rays have undergone a first Fermi cycle. Section 4 summarizes our results and provides some outlook. Details of the calculations are provided in Appendix A.

## 2 GENERAL CONSIDERATIONS

We carry out most of the discussion in the shock front rest frame, hence unless otherwise noted, all quantities are evaluated in this frame. We use the subscripts  $_{\text{u}}$  or  $_{\text{d}}$  to tag quantities measured in the upstream or in the downstream rest frame respectively.

### 2.1 Upstream diffusion length

In the upstream rest frame, cosmic rays can never stream too far ahead of a relativistic shock wave since this latter propagates towards upstream with velocity  $v_{\text{sh}} = \beta_{\text{sh}}c \approx c$  [the shock Lorentz factor  $\Gamma_{\text{sh}} \equiv (1 - \beta_{\text{sh}}^2)^{-1/2} \gg 1$ ]. Cosmic rays scatter on magnetic

turbulence upstream before they are caught back by the shock wave when their pitch angle  $\theta_{\text{u}} \sim 1/\Gamma_{\text{sh}}$  (Gallant & Achterberg 1999, Achterberg *et al.* 2001). Consequently, they can travel a distance  $\ell_{\text{cr|u}}$ , which may take the following values depending on the ratio of the Larmor radius  $r_{\text{L|u}}$  to the coherence length of the upstream magnetic field  $\lambda_{\text{c|u}}$  (Milosavljević & Nakar 2006):

- for small scale turbulence

$$\ell_{\text{cr|u}} \sim \frac{1}{\Gamma_{\text{sh}}^2} \frac{r_{\text{L|u}}^2}{\lambda_{\text{c|u}}} \quad (r_{\text{L|u}} \gg \Gamma_{\text{sh}} \lambda_{\text{c|u}}), \quad (1)$$

- for large scale turbulence

$$\ell_{\text{cr|u}} \sim \frac{r_{\text{L|u}}}{\Gamma_{\text{sh}}} \quad (r_{\text{L|u}} \ll \Gamma_{\text{sh}} \lambda_{\text{c|u}}). \quad (2)$$

Both regimes, short or large scale turbulence can be expected at some point, insofar as the excitation of the upstream magnetic field on short spatial scales is due to the streaming of the non-thermal particle population in the shock precursor. Indeed, cosmic rays of the first generation are to interact with a turbulent magnetic field ordered on large scales. However, provided the instability that they trigger grows fast enough, cosmic rays of the next generation will propagate in short scale turbulence. In reality, the situation is likely to be more complex as the process of particle propagation upstream and magnetic field generation are closely intertwined. The fact that the non-thermal population contains particles of different energies, which can stream at different distances from the shock front, should also play a significant role. In this respect, Keshtet *et al.* (2008) have observed that the upstream magnetic field is affected to greater distances as time goes on. This strongly suggests that higher energy cosmic rays are produced as time goes on, and that, by travelling farther in the upstream medium, they excite the turbulence at larger distances from the shock front.

In the discussion that follows, we estimate the growth of unstable modes in both the limits of small or large scale turbulence in order to remain as general as possible. Certainly the limit of large scale turbulence is more restrictive with respect to the growth of the instability, since the distance travelled upstream is significantly reduced with respect to that in small scale turbulence. Whichever limit prevails depends on the ratio of the short scale turbulent to the large scale (coherent) magnetic field strength, as discussed in Section 2.2. We also discuss the effect of higher energy cosmic rays on the growth rate.

It is important to emphasize that the distance that controls the growth of the instability is that between the shock front and the position of the particle, which is smaller than  $\ell_{\text{cr|u}}$  by a factor  $(1 - \beta_{\text{sh}}) \sim (2\Gamma_{\text{sh}}^2)^{-1}$ . In the following, we will need the expression for  $\ell_{\text{cr|sh}}$  (also noted  $\ell_{\text{cr}}$ ), i.e. the length scale of the cosmic-ray distribution as measured in the shock front rest frame. It can be calculated by transforming the upstream residence time  $t_{\text{r|u}} \approx \ell_{\text{cr|u}}/c$  in the shock front frame  $t_{\text{r|sh}} = t_{\text{r|u}}/\Gamma_{\text{sh}}$ , and then by rewriting in the expression obtained the upstream Larmor radius and coherence length in terms of their shock frame equivalent. In the perpendicular (or superluminal and ultra-relativistic) configuration of interest,  $r_{\text{L|sh}} \approx \Gamma_{\text{sh}}^{-2} r_{\text{L|u}}$ ,  $\lambda_{\text{c|sh}} \approx \Gamma_{\text{sh}}^{-1} \lambda_{\text{c|u}}$ . This boost of the coherence length is valid for wavenumber modes that are parallel to the shock normal; perpendicular wavenumber modes remain unchanged. In the following, we thus use the following expressions for  $\ell_{\text{cr}}$ :

- for small scale turbulence

$$\ell_{\text{cr}} \equiv \ell_{\text{cr|sh}} \approx \frac{r_{\text{L|sh}}^2}{\lambda_{\text{c|sh}}}, \quad (3)$$

- for large scale turbulence

$$\ell_{cr} \equiv \ell_{cr|sh} \simeq r_{L|sh} . \quad (4)$$

Below, we find a process of generation of intense magnetic disturbances at short spatial scales. The expected instabilities in all relevant cases generate disturbances with a coherence length  $\lambda_{c|u}$  between the minimal length  $l_{MHD} = c/\omega_{p,i}$  required for the validity of MHD description and the diffusion length  $\ell_{cr|u}$  of the cosmic rays, but with a preference for short scale, i.e.  $l_{MHD} \lesssim \lambda_{c|u} \lesssim \ell_{cr|u}$ . The minimal MHD length is:

$$l_{MHD} \equiv \beta_A r_{0|u} , \quad (5)$$

where  $\beta_A \equiv B_{0|u}/\sqrt{4\pi\rho_{0|u}c^2}$  denotes throughout this paper the Alfvén velocity (measured upstream) in units of  $c$ , and  $r_{0|u} = m_p c^2/eB_{0|u}$  is the Larmor radius of thermal protons in the upstream comoving frame. The above MHD scale is measured in the upstream plasma rest frame.

## 2.2 Requirements for successful Fermi acceleration

As discussed in Lemoine, Pelletier & Revenu (2006), a particle can execute a large number of Fermi cycles through the shock only if the turbulence coherence scale is much smaller than the Larmor radius (assuming no coherent magnetic field), in detail  $r_{L|u} \gg \lambda_{c|u}\Gamma_{sh}$  upstream, or  $r_{L|d} \gg \lambda_{c|d}$  as measured downstream.

The Fermi process becomes inoperative in the limit of large coherence length (when compared to the typical Larmor radius) since the cycle time becomes smaller than a coherence time hence the field is effectively regular and superluminal on a typical Fermi cycle. Conversely, the Fermi process will be operative provided either of the above inequalities is fulfilled, since the memory of the initial conditions at shock crossing is then erased by pitch angle diffusion in the short scale turbulence.

In the generic case of a ultra-relativistic superluminal shock, the above two conditions are actually related by the shock jump conditions, since the Larmor radius increases by  $\sim \Gamma_{rel}^2$  when going from downstream to upstream, while the coherence length increases by  $\sim \Gamma_{rel}$ . The quantity  $\Gamma_{rel}$  corresponds to the Lorentz factor of the downstream fluid as measured upstream, and in the case of a ultra-relativistic strong shock,  $\Gamma_{rel} \simeq \Gamma_{sh}/\sqrt{2}$  (Blandford & McKee 1976).

In the following, we describe the upstream and downstream fluids as comprising a large scale component  $\mathbf{B}_0$  and a short scale turbulent generated by some unspecified instability. In this case, Fermi acceleration will be efficient provided the short scale field has a sufficient amplitude as compared to  $B_0$ . We discuss this condition in the following.

### 2.2.1 Upstream motion

In this particular section, all quantities are evaluated in the upstream rest frame and we avoid using the notation  $|u$  out of clarity. We derive here the requirements on the amplitude of the short scale component of the magnetic field that would allow successful Fermi acceleration. Without loss of generality, we assume that the coherent component  $\mathbf{B}_0$  lies in the plane  $x-y$ , the  $x$  direction corresponding to the shock normal (oriented toward upstream infinity). We denote by  $\mathbf{b}$  the irregular component (whose amplitude is expressed in units of  $B_0$ ). The layout is pictured in Fig. 1.

The total field is thus written as  $\mathbf{B} = B_0(\mathbf{e} + \mathbf{b})$ , and the particle

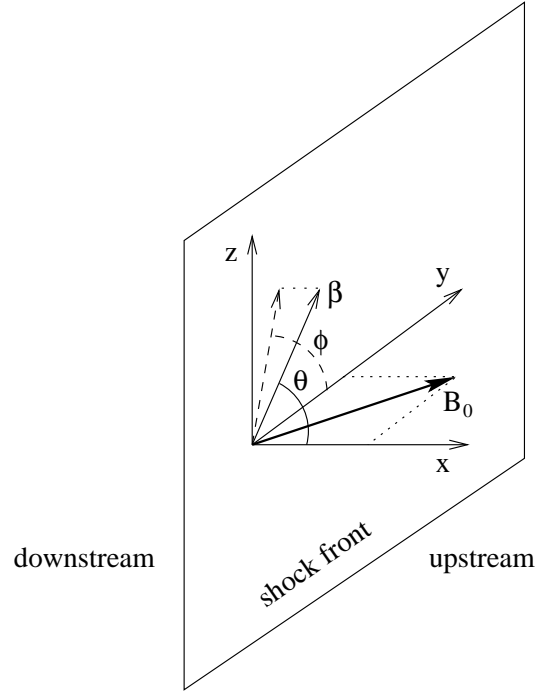


**Figure 1.** Schematic plot of the geometrical configuration in the upstream plasma rest frame. The coherent component  $\mathbf{B}_0$  lies in the  $x-y$  plane, with  $x$  pointing towards the shock normal, and  $(\theta, \phi)$  the angles of the particle velocity in this frame.

trajectory is governed by the following equation:

$$\frac{d\mathbf{b}}{dt} = \omega_{L,0} \mathbf{b} \times (\mathbf{e} + \mathbf{b}) , \quad (6)$$

with  $\omega_{L,0}$  denoting the Larmor frequency expressed relatively to  $B_0$ . We neglect the influence of any short scale time varying electric field  $\delta\mathbf{E}$  in the above equation of motion since  $\delta E/(B_0 b) \sim \omega/k \ll 1$ .

In order to quantify the return timescale and the condition for successful Fermi acceleration as a function of the amplitude of the random component of the magnetic field, it is useful to express this equation in terms of the angles  $\theta$  and  $\phi$ , which are defined as:  $\beta_x = \cos \theta$ ,  $\beta_y = \sin \theta \cos \phi$  and  $\beta_z = \sin \theta \sin \phi$ . These equations of motion read:

$$\dot{\theta} = \omega_{L,0} [(e_y + b_y) \sin \phi - b_z \cos \phi] , \quad (7)$$

$$\dot{\phi} = \omega_{L,0} \left[ -e_x - b_x + (e_y + b_y) \frac{\cos \phi}{\tan \theta} + b_z \frac{\sin \phi}{\tan \theta} \right] . \quad (8)$$

Rescaling the Larmor frequency with respect to  $e_y B_0$ , i.e. defining  $\omega_{L,y} \equiv e_y \omega_{L,0}$ , and noting that  $\theta \ll 1$  when the particle propagates upstream, the equations of motion for  $\theta$  and  $\phi$  can be rewritten as follows:

$$\begin{aligned} \dot{\theta} &\simeq \omega_{L,y} \sin(\phi) + \omega_{L,y} A \sin(\phi - \sigma) , \\ \dot{\phi} &\simeq \omega_{L,y} \frac{\cos \phi}{\theta} + \omega_{L,y} A \frac{\cos(\theta - \sigma)}{\theta} . \end{aligned} \quad (9)$$

The factors  $A$  and  $\sigma$  describe respectively the amplitude and the phase of the small scale magnetic field in the shock front plane, i.e.  $b_y = A \cos \sigma$  and  $b_z = A \sin \sigma$  (assuming isotropic turbulence). The amplitude  $A = \delta B/B_y$  is measured with respect to  $B_y$ .

One can extract from the above system the unperturbed trajec-

tory, i.e. assuming  $A = 0$ :

$$\cos \phi = \cos \phi_i \frac{\sin \theta_i}{\sin \theta}, \quad (10)$$

where values indexed with  $i$  are calculated at some initial time. Since entry into upstream corresponds to  $\cos \theta_i > \beta_{\text{sh}}$  hence  $\theta_i \lesssim 1/\Gamma_{\text{sh}}$ , and exit from upstream corresponds to  $\theta \gtrsim 1/\Gamma_{\text{sh}}$ , the above equation suggests that  $\phi$  is driven to an angle close to  $\pm\pi/2$ . The sign is given by the sign of  $e_y$ ; for  $e_y > 0$ , it is  $+\pi/2$ . This region lies opposite to that which allows return to the shock when the particle travels downstream (see Lemoine, Pelletier & Revenu 2006), hence Fermi cycles cannot be completed. It is important to note that this unperturbed trajectory is executed on a timescale  $t_{\text{unpert}} \simeq r_{\text{L},y}/(\Gamma_{\text{sh}}c)$  (where  $r_{\text{L},y} = c/\omega_{\text{L},y}$ ).

The noise term comes from the random phase  $\sigma$  (assuming isotropic turbulence in the shock front plane, an assumption that can be relaxed). Therefore the trajectory deviates from the unperturbed trajectory to linear order by  $(\Delta\phi, \Delta\theta)$ , whose variance increases linearly with time:

$$\begin{aligned} \langle \Delta\phi^2 \rangle &\simeq \frac{1}{3} A^2 \frac{\omega_{\text{L},y}^2}{\theta^2} \tau_c \Delta t, \\ \langle \Delta\theta^2 \rangle &\simeq \frac{2}{3} A^2 \omega_{\text{L},y} \tau_c \Delta t. \end{aligned} \quad (11)$$

Note that the above equation does not contain all the terms driving the variance of  $\phi$  and  $\theta$ : it neglects term of the form  $\int dt_1 dt_2 \langle \Delta\phi(t_1) \Delta\phi(t_2) \rangle$  and similarly in  $\Delta\theta$ . However, these terms are smaller by  $\mathcal{O}(A^2)$  as compared to those above, hence they can be neglected in a first approximation (we will find  $A \gg 1$  further below).

In the absence of the regular driving term in the equations of motion (i.e. when  $B_y = 0$ ), return occurs over a timescale  $t_{\text{diff}} \simeq (\Gamma_{\text{sh}}^2 A^2 \omega_{\text{L},y}^2 \tau_c)^{-1}$ . Noise dominates over the unperturbed trajectory if  $\langle \Delta\theta^2 \rangle \gtrsim \theta^2$ , where  $\theta$  indicates the unperturbed trajectory. This inequality must be satisfied within a (return) timescale  $t_{\text{unpert}}$  otherwise the particle will have exited from upstream (along the weakly perturbed unperturbed trajectory) before the noise could overcome the unperturbed driving force. This implies:

$$A^2 \gtrsim \frac{1}{\Gamma_{\text{sh}} \omega_{\text{L},y} \tau_c}. \quad (12)$$

If one defines the Larmor radius  $r_{\text{L}}$  measured with respect to the total magnetic field,  $r_{\text{L}} = c[(A^2 + 1)^{1/2} \omega_{\text{L},0}]^{-1}$ , hence  $r_{\text{L}} \simeq c/(A\omega_{\text{L},y})$  when  $A \gg 1$ , the former inequality amounts to:

$$A \gtrsim \frac{r_{\text{L}}}{\Gamma_{\text{sh}} \lambda_c}. \quad (13)$$

If this inequality is satisfied, then one can check that  $\langle \Delta\phi^2 \rangle^{1/2} \sim \mathcal{O}(1)$  on a return timescale  $t_{\text{diff}}$ , which implies that the return directions are isotropized in the shock front plane. Fermi acceleration should then be efficient (provided the return probability to the shock as calculated downstream is also isotropic in  $\phi$ , see below).

An interesting implication of the above is to restrict Fermi acceleration to a rather limited range of Larmor radii:

$$\Gamma_{\text{sh}} \lambda_c \lesssim \bar{r}_{\text{L}} \lesssim A \Gamma_{\text{sh}} \lambda_c. \quad (14)$$

Very high values of the amplification factor are thus required to produce powerlaw spectra over a large dynamic range.

### 2.2.2 Downstream motion

All quantities in this subsection are evaluated in the downstream rest frame. In this frame, the coherent magnetic field is nearly fully

aligned with the  $y$ -axis, and we assume indeed that  $\mathbf{B}_0 = B_0 \mathbf{y}$ . It is useful to study the evolution of the velocity components perpendicular ( $\beta_{\perp}$ ) and parallel ( $\beta_{\parallel}$ ) to the direction of  $\mathbf{B}_0$ :  $\beta_{\parallel} \equiv \beta_y$ ,  $\beta_{\perp}^2 = \beta_x^2 + \beta_z^2$ . The equations of motion for the velocity  $\beta$  can then be written:

$$\begin{aligned} \dot{\beta}_{\perp} &= \omega_{\text{L},0} \frac{\beta_{\parallel}}{\beta_{\perp}} (\beta_x b_z - \beta_z b_x) \\ \dot{\beta}_{\parallel} &= \omega_{\text{L},0} (\beta_z b_x - \beta_x b_z). \end{aligned} \quad (15)$$

One can check that  $\beta_{\parallel} \dot{\beta}_{\parallel} + \beta_{\perp} \dot{\beta}_{\perp} = 0$  as it should since  $\beta$  is conserved. The unperturbed trajectory for the couple of variables  $(\beta_{\parallel}, \beta_{\perp})$  is trivial, i.e.  $\beta_{\perp,0} = \text{const.} = \beta_{\perp,i}$  and  $\beta_{\parallel,0} = \text{const.} = \beta_{\parallel,i}$ . Return may occur or not, depending on these initial velocity components; if it occurs, it does so on a timescale  $t_{\text{unpert}} \simeq r_{\text{L},0}/c$  (Lemoine, Pelletier & Revenu 2006).

Since  $b_x$  is not compressed through shock crossing,  $b_x/b_z \sim 1/\Gamma_{\text{sh}}$  for isotropic upstream turbulence, hence this component can be neglected. Integrating the above equations to calculate the squared perpendicular displacement, one finds:

$$\begin{aligned} \langle \Delta x_{\perp}^2 \rangle &= \int_0^t dt_1 \int_0^t dt_2 \langle \beta_{\perp}(t_1) \beta_{\perp}(t_2) \rangle \\ &\simeq \omega_{\text{L},0}^2 \frac{\beta_{\parallel,i}^2}{\beta_{\perp,i}^2} \int_0^t dt_1 \int_0^t dt_2 \int_0^{t_1} dt_3 \int_0^{t_2} dt_4 \\ &\quad \beta_{x,0}(t_3) \beta_{x,0}(t_4) \langle b_z(t_3) b_z(t_4) \rangle \\ &\simeq \omega_{\text{L},0}^2 \frac{\beta_{\parallel,i}^2}{\beta_{\perp,i}^2} \int_0^t dt_1 \int_{t_1}^t dt_2 \int_0^{t_1} dt_3 \frac{A^2}{3} \tau_c \beta_{x,0}^2(t_3) \\ &\simeq \frac{A^2}{3} \omega_{\text{L},0}^2 \tau_c \frac{\beta_{\parallel,i}^2}{\beta_{\perp,i}^2} P(t). \end{aligned} \quad (16)$$

In the above equation,  $\beta_{x,0}(t)$  represents the unperturbed trajectory:  $\beta_{x,0} = \beta_{x,i} \cos(\omega_{\text{L},0} t) - \beta_{z,i} \sin(\omega_{\text{L},0} t)$ . The function  $P(t)$  contains powers of  $t$  up to  $t^3$ , as well as sine and cosine functions of  $2\omega_{\text{L},0} t$ ; its dimension is that of  $c^2 \omega_{\text{L}}^{-3}$ . Noise will then dominate over the unperturbed trajectory  $x_{\perp,0} = \beta_{\perp,i} c t$  over a unperturbed return timescale if:

$$A^2 \gtrsim \frac{1}{\omega_{\text{L},0} \tau_c}, \quad (17)$$

or, equivalently:

$$A \gtrsim \frac{r_{\text{L}}}{\lambda_c}. \quad (18)$$

As before,  $r_{\text{L}}$  denotes the Larmor radius measured with respect to the total magnetic field. This condition on  $A$  is very similar to that obtained upstream, since  $r_{\text{L},\text{lu}} \sim \Gamma_{\text{sh}}^2 r_{\text{L},\text{d}}$  and  $\lambda_{\text{cl},\text{lu}} \sim \Gamma_{\text{sh}} \lambda_{\text{cl},\text{d}}$ , while  $A_{\text{lu}} \simeq A_{\text{d}}$ .

According to the above analysis, and following Lemoine, Pelletier & Revenu (2006), phase mixing should be sufficiently large to erase all dependence on the phase of the velocity vectors, hence Fermi acceleration should be fully operative, if either one of the above conditions on  $A$  is satisfied.

It is interesting to discuss the above results in light of recent Monte Carlo numerical simulations of relativistic Fermi acceleration in the presence of short scale turbulence (Niemi, Ostrowski & Pohl 2006). These authors have investigated the efficiency of the Fermi process for various turbulence configurations, including a coherent magnetic field, a long wave turbulence and a short scale component. They confirm that Fermi acceleration is not operative if  $\delta B/B = 0$ , but find that a spectrum can develop over about two orders of magnitude when  $\delta B/B = 80$  (see their Fig. 1). The high

energy break can be directly interpreted as the energy at which the above inequality Eq. (18) is no longer fulfilled. Beyond that point, the spectrum steepens and the Fermi process becomes inoperative. Interestingly, these authors also show that if the pitch angle scattering amplitude in the short scale turbulence is independent of energy, the break disappears and the spectrum continues without bound. This is also expected, insofar as the break that is determined by Eq. (18) stems from the fact that the scattering time in the short scale turbulence scales as the square of the Larmor time whereas the unperturbed trajectory in the background field depends linearly on the Larmor time. Assuming a constant pitch angle scattering amplitude in the notations of Niemiec, Pohl & Ostrowski (2006) implies that the two scattering timescales evolve in the same way, hence if short scale turbulence suffices to isotropize directions at a given energy, it will do so at all energies.

In order to produce powerlaw spectra over a large dynamic range, it is thus necessary to reach an amplification factor  $\delta B/B$  as large as possible, since this ratio determines the dynamic range of particle energies. Interestingly, the afterglow modeling of gamma-ray bursts suggest that indeed, the upstream and downstream magnetic fields have been amplified by a large factor. In the range of energies in which Fermi acceleration is operative, it is likely that the spectral index would be equal to the so-called canonical value  $s = 2.3$ , although the generality of this prediction for different shapes of the 3d turbulence spectrum remains to be studied. The results of Niemiec, Ostrowski & Pohl (2006) cannot be used to infer this spectral index, since they have restricted their analysis to values of  $\delta B/B < 100$ , and the spectral indices they report have been measured beyond the break energy. Techniques developed in Lemoine & Pelletier (2003), Lemoine & Revenu (2006) are particularly suited to study this problem and calculations are underway.

### 3 INSTABILITIES AT PERPENDICULAR SHOCK WAVES

The magnetic field in the shock front  $B_{\text{sh}}$  is related to the magnetic field in the upstream frame  $B_{\text{lu}}$  and the associated electric field  $E_{\text{lu}}$  through the Lorentz transform:

$$\begin{aligned} B_{\parallel\text{sh}} &= B_{\parallel\text{lu}} \\ \mathbf{B}_{\perp\text{sh}} &= \Gamma_{\text{sh}} (\mathbf{B}_{\perp\text{lu}} - \beta_{\text{sh}} \times \mathbf{E}_{\perp\text{lu}}) . \end{aligned} \quad (19)$$

To zeroth order, the electric field in the upstream plasma frame vanishes, hence the magnetic field in the shock front frame is mostly perpendicular unless  $\mathbf{B}_{\text{lu}}$  is aligned along the shock normal to within an angle  $\sim \mathcal{O}(1/\Gamma_{\text{sh}})$  (subluminal shock). It then suffices to consider the fully perpendicular situation with  $B_{\parallel\text{sh}} = 0$ .

The cosmic rays stream ahead of the shock wave, carrying a net charge density  $\rho_{\text{cr}}$  which will induce a counteracting charge density  $\rho_{\text{pl}}$  in the background plasma. Note that the cosmic rays do not induce an electrical current at zeroth order in the shock front frame, only a net charge density. Since we consider the generation of short scale turbulence, we neglect the cosmic ray response to this short scale turbulence other than its effect on the cosmic ray distribution scale  $\ell_{\text{cr}}$ . For simplicity, we approximate the cosmic-ray charge profile with a top-hat distribution.

As usual, we search for a stationary regime which serves as a basis for perturbing the equations in the time-dependent regime. The details of the calculations are provided in Appendix A for both stationary and time dependent quantities. In particular, the stationary regime exhibits the following set-up:

$$\mathbf{B} = B_y \mathbf{e}_y, \quad \mathbf{u} = u_x \mathbf{e}_x + u_z \mathbf{e}_z . \quad (20)$$

Recalling that the shock normal is directed along  $x$ ,  $u_x \simeq -\Gamma_{\text{sh}}\beta_{\text{sh}}$  characterizes the velocity of the upstream inflowing through the front. The velocity component  $u_z$  along the front is small compared to  $u_x$ , but its shear  $\partial_x u_z$  cannot be neglected (see Appendix A).

#### 3.1 Linear analysis of the reduced system

The complete system that governs the linear evolution is of seventh order (see Appendix A) and thus rather involved. Nevertheless, it remains possible to derive the main results since the Lorentz transform from the upstream comoving frame to the shock front frame dominates the MHD propagation effects when the wave scale is ‘‘not too small’’, as will be made more precise in a next subsection. In other words, the instability growth rates can be derived to lowest order by assuming vanishing Alfvén and sound velocities. We have verified that the analysis of the system including  $\beta_A$  and  $\beta_s$  (but neglecting terms in  $u_z$ ) does not modify the growth rates obtained further below.

One should point out that electromagnetic waves with dispersion relation  $\omega_{\text{lu}}(\mathbf{k}_{\text{lu}})$  are Lorentz transformed into waves with dispersion relation:

$$\omega \simeq \beta_{\text{sh}} c k_x + \mathcal{O}\left(\frac{k_{y,z}}{\Gamma_{\text{sh}}}\right) . \quad (21)$$

In particular, for Alfvén waves, the next term on the r.h.s. is  $\beta_A k_y c / \Gamma_{\text{sh}}$ . Note that the Alfvén velocity is always expressed in the upstream plasma rest frame, i.e.  $\beta_A = B_{y\text{lu}} / \sqrt{4\pi\rho_{\text{lu}}c^2}$ . Therefore it suffices in what follows to consider the limit  $k_z \rightarrow 0$ . The limit  $k_y \rightarrow 0$  can also be considered but it appears more restrictive, because it limits the analysis to the evolution of upstream magnetosonic modes. We will thus consider both cases  $k_y = 0$  and  $k_y$  finite. Of course, one can use Fourier analysis without mode coupling as long as the spatial dependence of the system coefficients can be neglected, in agreement with our previous approximations, and in particular, that the cosmic ray charge density is modeled as a step function. In the shock front rest frame, the physical picture of the instability is then as follows. Impinging electromagnetic waves propagate in vacuum beyond the length scale  $\ell_{\text{cr}}$  which characterizes the spatial distribution of cosmic rays upstream of the shock front. For  $0 < x < \ell_{\text{cr}}$ , the presence of the cosmic-ray charge density induces a short scale instability. Hence we consider electromagnetic waves and seek a solution in Fourier space with  $\omega$  set by its vacuum dispersion relation, but with a complex  $k_x$  characterizing the amplification in the charge layer  $0 < x < \ell_{\text{cr}}$ .

In this perpendicular configuration, the return current (in the upstream frame) is not responsible for a supplementary tension effect, but for a supplementary compression effect. A  $b_y$  perturbation leads to a supplementary vertical (i.e. along  $z$ ) compression that can push like the kinetic compression. If we consider a spatial modulation along the mean field ( $k_y \neq 0$ ), a vertical perturbation  $b_z$  generates a supplementary compression in the direction of the mean field that can push in phase with the kinetic compression as well.

For large  $\Gamma_{\text{sh}}$  even with  $k_z \neq 0$ , the system reduces to fourth order and can be expressed as the coupling between the propagation of the vertical perturbed motion  $\delta u_z$  and the propagation of kinetic compression  $\delta w/w$ , where  $w \equiv \rho_{\text{u}}c^2$  is the relativistic proper enthalpy density of the cold upstream plasma. The system of the two coupled equations can be expressed using the system of Eqs. (A18),(A19),(A21) in the limit  $\beta_A \rightarrow 0, \beta_s \rightarrow 0$ . In particular in this limit, one notes that  $b_x \approx 0$ .

Then one obtains a single equation for  $\delta u_z$  (see Ap-

pendix A2.2) where derivatives  $\partial_z$  cancel out and where the derivative of  $u_z$  is inserted, its second derivative being neglected (we also assume  $\beta_{\text{sh}} = 1$  in the coefficients):

$$\hat{D}^4 \delta u_z - (\kappa^2 + u_z \kappa \partial_x) \hat{D}^2 \delta u_z + \Gamma_{\text{sh}} \kappa^2 \partial_x \hat{D} \delta u_z + \Gamma_{\text{sh}}^2 \kappa^2 \partial_x^2 \delta u_z = 0. \quad (22)$$

The differential operator  $\hat{D}$  is defined by  $\hat{D} = \Gamma_{\text{sh}} (c^{-1} \partial_t - \beta_{\text{sh}} \partial_x)$ . For a detailed understanding of the instabilities one has to notice that the charge is not completely screened by the plasma as a supplementary electric field is generated along the flow (i.e. oriented towards  $-x$ ):  $E_x = u_z B_y / \Gamma_{\text{sh}}$ , along with a sheared vertical motion  $u_z$  such that  $\partial_x u_z = \kappa$  (see Appendix A). The instabilities stem from this sheared motion. The parameter  $\kappa$ , which carries the dimension of a wavenumber, is defined in Eq. (A23). To our present order of approximation, it can be expressed as:

$$\kappa \equiv \frac{\rho_{\text{cr}} B_y}{\Gamma_{\text{sh}} W}. \quad (23)$$

Note that both  $\rho_{\text{cr}}$  and  $B_y$  are here evaluated in the shock front frame. In the front frame, the parameter  $\kappa$  appears divided by  $\Gamma_{\text{sh}}$ , hence we introduce  $k_* \equiv \kappa / \Gamma_{\text{sh}}$ .

The reduced form of the equation (see Appendix A2.2) clearly shows the ordering (by setting  $\hat{D} = k_x \beta_{\text{sh}} \Gamma_{\text{sh}} \tilde{D}$ ,  $\delta u_z = \beta_{\text{sh}} \Gamma_{\text{sh}} \tilde{u}_z$ ):

$$\tilde{D}^4 \tilde{u}_z - \left( \frac{k_*^2}{k_x^2} + \frac{u_z}{\Gamma_{\text{sh}}} \frac{k_* \partial_x}{k_x^2} \right) \tilde{D}^2 \tilde{u}_z + \frac{k_*^2 \partial_x}{k_x^3} \tilde{D} \tilde{u}_z + \frac{k_*^2}{k_x^4} \partial_x^2 \tilde{u}_z = 0 \quad (24)$$

The inhomogeneity is contained in  $\kappa^2$  that vanishes at large distance from the shock. At infinity  $\hat{D} \delta u_z = 0$ , which implies that for a mode having a specified  $k_x$ , the pulsation  $\omega = \beta_{\text{sh}} k_x c$ , as expected. In the precursor where  $\kappa^2 \neq 0$ , we follow this mode characterized by its frequency and look at the modification of its spatial behavior. As explained above, we solve this equation by setting  $c^{-1} \partial_t \mapsto i \beta_{\text{sh}} k_x$ ,  $\partial_x \mapsto i k_x (1 - \varepsilon)$ , so that  $\hat{D} \mapsto i k_x \beta_{\text{sh}} \Gamma_{\text{sh}} \varepsilon$  ( $\tilde{D} \mapsto i \varepsilon$ ), where  $\varepsilon$  is a complex number, the imaginary part of which characterizes the growth rate. It is obtained by solving the algebraic equation:

$$\varepsilon^4 + 2 \frac{k_*^2}{k_x^2} \varepsilon^2 - \frac{k_*^2}{k_x^2} \varepsilon - \frac{k_*^2 k_y^2}{k_x^4} + i \frac{u_z}{\Gamma_{\text{sh}}} \frac{k_*}{k_x} (1 - \varepsilon) \varepsilon^2 = 0 \quad (25)$$

Actually, because  $\varepsilon$  is small, the equation can be simplified to:

$$\varepsilon^4 - \frac{k_*^2}{k_x^2} \varepsilon - \frac{k_*^2 k_y^2}{k_x^4} = 0. \quad (26)$$

The contribution in  $u_z$  introduces a small correction to the real part of the roots (most  $u_z$  contributions can be canceled out by a frame transformation, but that correction cannot be canceled out because it corresponds to the electric field component  $E_x$ ).

### 3.1.1 Analysis of the case $k_y = 0$

Let us first analyze the case  $k_y = 0$ , or less restrictively for  $k_y^2 \ll |\varepsilon^2| k_x^2$ . This is a pure magneto-sonic compression with  $\mathbf{b}$  along the mean field. One gets the following three roots:

$$\varepsilon \simeq - \left( \frac{k_*}{k_x} \right)^{2/3} \left( -1, \frac{1 \pm i \sqrt{3}}{2} \right), \quad (27)$$

One obtains an instability spatial growth rate  $\gamma_x = \text{Im}(k_x \varepsilon)$  that increases with large  $k_x$ .

$$\gamma_x = \frac{\sqrt{3}}{2} k_*^{2/3} k_x^{1/3} \quad (k_x \gg k_*). \quad (28)$$

Thus the characteristic wave number associated with the charge in this problem of magneto-sonic wave propagation is  $k_* \equiv \kappa / \Gamma_{\text{sh}}$ .

### 3.1.2 Analysis of the case $k_y \neq 0$

With  $k_y \neq 0$ , one recovers the previous growth rate if  $k_y \ll k_*^{1/3} k_x^{2/3}$ , while for  $k_y \gg k_*^{1/3} k_x^{2/3}$  one derives :

$$\varepsilon \simeq \left( \frac{k_y k_*}{k_x^2} \right)^{1/2} (1, -1, i, -i), \quad (29)$$

or, equivalently:

$$\gamma_x \simeq (k_y k_*)^{1/2} \quad (k_y \gg k_*^{1/3} k_x^{2/3}). \quad (30)$$

The spatial growth rates are thus  $\gamma_x \sim (k_*^2 k_x)^{1/3}$  and  $(k_* k_y)^{1/2}$  respectively. Remarkably they are independent of  $k_z$  that can be chosen arbitrarily, provided it remains small compared to  $k_x$  for the consistency of the derivation.

### 3.1.3 Comparison to MHD and cosmic-ray length scales

One should compare the scale defined by  $k_*$  to the smallest scale  $l_{\text{MHD}}$  for our MHD description. Note that this length scale is defined in the comoving upstream frame. Since  $k_{x|\text{u}} \simeq k_x / \Gamma_{\text{sh}}$  while  $k_{y|\text{u}} \simeq k_y$ , it suffices to require  $k_* l_{\text{MHD}} < 1$  to ensure that there exist modes in the MHD range with  $k > k_*$ . One obtains:

$$k_* l_{\text{MHD}} = \frac{n_{\text{cr}} e B_y}{\Gamma_{\text{sh}}^2 W} \beta_A r_{0|\text{u}} \quad (31)$$

which can be rewritten in terms of the fraction  $\xi_{\text{cr}}$  of (downstream) shock internal energy converted into (downstream) cosmic ray energy:

$$\xi_{\text{cr}} \equiv \frac{e_{\text{cr|d}}}{4 \Gamma_{\text{sh}}^2 W}. \quad (32)$$

To this effect, we assume that the accelerated population can be described as a power-law of index  $-s$  and minimum momentum  $p_{\text{min}}$ , so that:

$$n_{\text{cr}} \simeq \frac{|1-s|}{|2-s|} \frac{e_{\text{cr}}}{p_{\text{min}} c}. \quad (33)$$

This equation assumes  $s > 2$ ; if  $s = 2$ , then  $|2-s|$  should be replaced by  $\log(p_{\text{max}}/p_{\text{min}})$ . Since  $e_{\text{cr|d}} \sim e_{\text{cr|sh}}$  (as  $\Gamma_{\text{sh|d}} = \sqrt{9/8}$  for a strong ultra-relativistic shock), one obtains:

$$k_* l_{\text{MHD}} \simeq 4 \frac{|1-s|}{|2-s|} \xi_{\text{cr}} \beta_A \frac{r_{0|\text{u}}}{r_{\text{min}|\text{u}}} \Gamma_{\text{sh}}^2. \quad (34)$$

Here  $r_{\text{min}|\text{u}}$  denotes the minimum Larmor radius of the accelerated population, as measured upstream. The typical energy of the first generation of cosmic rays is  $\Gamma_{\text{sh}}^2 m_p c^2$ , so that  $r_{\text{min}|\text{u}} \sim \Gamma_{\text{sh}}^2 r_{0|\text{u}}$ . Therefore

$$k_* l_{\text{MHD}} \sim 4 \frac{|1-s|}{|2-s|} \xi_{\text{cr}} \beta_A \ll 1. \quad (35)$$

Thus  $k_*$  defines an MHD scale.

In order for the instability to be efficient, one must also require  $\gamma_x \ell_{\text{cr}} \gg 1$ , which is a non-trivial requirement in view of the restricted value of  $\ell_{\text{cr}}$ . One finds:

$$\gamma_x \ell_{\text{cr}} \simeq 4 \frac{|1-s|}{|2-s|} \frac{\gamma_x}{k_*} \xi_{\text{cr}} g, \quad (36)$$

with  $g \equiv 1$  for large scale turbulence, and  $g \equiv r_{0|\text{u}} / \lambda_{\text{cl}|\text{u}}$  for short scale turbulence. In the latter case, one may assume  $\lambda_{\text{cl}|\text{u}} \simeq l_{\text{MHD}}$ , as suggested by the fact that the growth rate increases with  $k$ , so that  $g \sim 1/\beta_A$ . Then, in both cases, the total growth is presumably much larger than unity if  $\xi_{\text{cr}}$  is not too small and  $k_x, k_y$  sufficiently

large as compared to  $k_*$ . Hence even the first generation of cosmic rays is able to destabilize the upstream magnetic field on the shortest scales. The effect of the high energy part of the accelerated population will be addressed shortly.

As mentioned, the study of the more extended system including the contribution of the terms involving the Alfvénic and sonic contributions (but neglecting terms of order  $u_z$  in the system) confirms the results above for the growth rates, provided  $\beta_A \ll 1$  and  $\beta_s \ll 1$ .

### 3.1.4 Magneto-sonic saturation

One can estimate the amplitude of the various components in terms of  $b_y$ . It has already been mentioned that  $|b_x| \ll |b_y|$ ,

$$b_y \simeq \frac{\beta_{\text{sh}}}{\Gamma_{\text{sh}}} \delta u_x \quad (37)$$

and

$$b_z \simeq -\frac{1}{\kappa} \partial_y \delta u_x. \quad (38)$$

Thus we find that  $b_z$  may achieve a large amplitude, because

$$b_z \simeq -\frac{\Gamma_{\text{sh}}}{\kappa \beta_{\text{sh}}} \partial_y b_y. \quad (39)$$

In the frame of linear theory, the saturation level of these magneto-sonic instabilities is simply estimated by the fact that the compression has a limited amplitude  $|\delta w/w| < 1$ . Defining the power spectrum of  $b_y$  and  $b_z$  per log interval of wavenumber  $\mathcal{P}_{b_y} \equiv (k^3/2\pi^2) |\tilde{b}_y|^2$  in terms of the Fourier component  $\tilde{b}_y$  and similarly for  $\mathcal{P}_{b_z}$  in terms of  $\tilde{b}_z$ , one derives from Eq. (A33):

$$\mathcal{P}_{b_y}^{1/2} \leq \frac{k_*^2}{|\varepsilon^2 k_x^2 + 2k_x^2|} \quad (40)$$

and

$$\mathcal{P}_{b_z}^{1/2} = \frac{k_y}{k_*} \mathcal{P}_{b_y}^{1/2}. \quad (41)$$

Note that the power spectrum is normalized to the ratio of amplitude of the turbulent (small scale) component to the coherent  $B_0$ . Consider the first branch of the instability, given by Eq. (28) which applies in the limit  $k_x \gg k_*$ ,  $k_y \ll k_*^{1/3} k_x^{2/3}$ . There one can show that  $\mathcal{P}_{b_y}^{1/2}$  saturates at a value of order  $(k_x/k_*)^{-2/3} \ll 1$ , but  $\mathcal{P}_{b_z}^{1/2}$  saturates at a value of order unity when  $k_y \sim k_*^{1/3} k_x^{2/3}$ . For the second branch, given in Eq. (30) and which applies in the limit  $k_y \gg k_*^{1/3} k_x^{2/3}$ , one finds that  $\mathcal{P}_{b_y}^{1/2}$  saturates at a value of order  $k_*/k_y \ll 1$ , but again  $\mathcal{P}_{b_z}^{1/2}$  saturates at a value unity. This moderate saturation level can be directly traced back to the saturation of these compressive modes at the linear level  $|\delta w/w| \sim 1$ . As discussed in Sec. 2.2, such a level  $\delta B/B_0 \sim 1$  should not allow a powerlaw spectrum to develop through Fermi acceleration.

Nevertheless, our present analytical description is by definition limited to the linear regime. It would certainly be interesting to pursue the calculations using numerical simulations as one could expect that the holes produced in the plasma would widen with the growing magnetic pressure inside and that the density excesses become spikes. Thus one might reasonably expect the generation of many local small magneto-sonic shocks that are absorbed by the main ultra-relativistic shocks, with the reconversion of some amount of cosmic-ray energy into thermal energy in the precursor.

The previous discussion has focused on the role played by the first generation of cosmic rays, since higher energy cosmic rays

can only be present if acceleration to smaller energies has been completed. However it is easy to verify that, if highest energy cosmic rays are present in the shock precursor, they are bound to play a dominant role in the amplification of the magnetic field, most notably because the length scale of the cosmic ray distribution increases as  $r_L^2$ . For instance, at a distance  $x$  from the shock front where only cosmic rays of momentum larger than  $p_*$  can be found, the critical wavenumber for the instability reads for  $s > 2$  ( $s$  spectral index of the accelerated population):

$$k_* = k_{*,0} \left( \frac{p_*}{p_{*,0}} \right)^{1-s}, \quad (42)$$

where  $k_{*,0}$  denotes the same wavenumber evaluated for the whole cosmic-ray distribution, and  $p_{*,0}$  denotes the minimum momentum of the cosmic ray distribution at the shock front. Consequently, if  $\gamma_x \propto k_*^a$ , with  $a = 2/3$  or  $1/2$  for the two branches of the instability obtained above:

$$\gamma_x \ell_{\text{cr},*} = \left( \frac{p_*}{p_{*,0}} \right)^{b+a(1-s)} \gamma_{x,0} \ell_{\text{cr}}, \quad (43)$$

with  $b = 1$  for large scale turbulence,  $b = 2$  for short scale turbulence. Here as well,  $\gamma_{x,0}$  should be understood as the growth rate derived previously for the whole cosmic-ray distribution. This product grows with increasing  $p_*/p_{*,0}$  provided  $s < (b+a)/a$ , i.e.  $s < 8$  ( $b = 2, a = 2/3$ ), or  $s < 5$  ( $b = 2, a = 1/2$ ), or  $s < 5/2$  ( $b = 1, a = 2/3$ ) or finally  $s < 3$  ( $b = 1, a = 1/2$ ). These inequalities are likely to be fulfilled. Finally, the product  $k_* \ell_{\text{MHD}}$  scales as  $(p_*/p_{*,0})^{1-s}$  hence decreases if  $s > 1$ . This also means the typical scale of the instability increases with increasing  $p_*/p_{*,0}$ .

Of course, the above implicitly ignores the spatial dependence of  $B$ , but it suggests that amplification through the streaming of the highest energy part of the cosmic ray distribution will seed much more efficiently the magnetic field amplification.

### 3.1.5 Non-existence of an incompressible instability

Since the above compressive instabilities appear to saturate at a level too small ( $\delta B/B \sim 1$ ) to allow Fermi acceleration over a broad range of energies, the possible existence of non-compressive instability becomes crucial. One can search for such modes by selecting the wave vectors accordingly, in which case the reduced system becomes:

$$\begin{aligned} \tilde{D}^2 \tilde{u}_z - \left( \frac{k_z^2}{k_x^2} + \frac{k_* \partial_z}{k_x^2} + \frac{u_z}{\beta_{\text{sh}} \Gamma_{\text{sh}}} \frac{k_* \partial_x}{k_x^2} \right) \tilde{u}_z + \frac{k_*}{k_x} &= 0 \\ \frac{k_* \partial_x}{k_x^2} \tilde{D} \tilde{u}_z - \frac{k_* \partial_y^2}{k_x^3} \tilde{u}_z - \frac{\partial_z}{k_x} \tilde{D}^2 \tilde{u}_z &= 0 \end{aligned} \quad (44)$$

It is easy to verify that this system possesses no unstable solution but only damped solutions. Hence incompressible unstable modes do not exist in this MHD description.

## 4 CONCLUSIONS

In this study, we have examined the amplification of a pre-existing magnetic field upstream of an ultra-relativistic shock wave. We have assumed that the magnetic field is fully perpendicular to the shock normal in the shock front frame, as generally expected in the ultra-relativistic limit  $\Gamma_{\text{sh}} \gg 1$ . In the shock frame, the cosmic rays do not induce any current at zeroth order, only a net charge density, which is partly screened by the inflowing plasma. This charge distribution then triggers an instability on very short spatial scales,

with a growth rate increasing with the wavenumber. Cosmic rays do not respond to this amplification as it takes on scales much shorter than the typical Larmor radius.

It is important to stress that these instabilities are of a different nature than the resonant or non-resonant instability studied by Bell (2004) in the case of a non-relativistic parallel shock wave, most notably because they are essentially *compressive*. Since density depletions are naturally limited, our linear analysis indicates that these instabilities saturate at a moderate level of amplification,  $\delta B/B_0 \sim 1$ . Furthermore, there is no unstable incompressible mode within the present MHD approximation which could provide a higher level of amplification. Therefore, we conclude that, within the framework of ideal MHD, instabilities at ultra-relativistic magnetized shock waves appear limited in their efficiency.

Such instabilities cannot therefore account for the degree of amplification that has been inferred from the modeling of the afterglow radiation of gamma-ray bursts. We have also argued in Section 2.2 that the ratio  $\delta B/B_0$  sets the dynamic range of energies over which powerlaw spectra can be produced through Fermi acceleration. The present instabilities thus cannot allow successful Fermi acceleration. Nevertheless, it would certainly be useful to pursue the present investigation with dedicated numerical simulations, which would allow one to go beyond the present linear approximation and study whether non-linear effects can push the small scale magnetic field to higher values.

If the standard interpretation of gamma-ray burst afterglows as the synchrotron light of electrons accelerated at the forward shock (but see Uhm & Beloborodov 2006, Genet, Daigne & Mochkovitch 2007 for recent alternatives involving the reverse shock) holds, one is led to conclude that some other instability is able to amplify the upstream magnetic field on short spatial scales, or that some other form of acceleration mechanism is operating (see for instance Hoshino 2008 for an alternative involving radiative pressure effects). The present work indicates that such cosmic ray induced instabilities would involve non-MHD effects. The short spatial scales  $\lambda_c \ll r_L/\Gamma_{\text{sh}}$  required are in conflict with the usual synchrotron resonance between cosmic rays and MHD waves; this remark is actually one of the motivation of the present work in a full MHD framework. However, one cannot rule out that other types of resonance could become relevant and yet involve incompressible modes, such as Alfvén waves. One promising instability, currently under study, involves a Cerenkov resonance ( $\omega = k_x c$ ) between plasma waves and the cosmic ray beam, generating a modified two stream instability. The growth rates appear quite promising and the details will be given in a forthcoming article.

## APPENDIX A: BACKGROUND AND PERTURBED QUANTITIES FOR PERPENDICULAR SHOCK WAVES

### A1 Stationary regime

In the shock front frame, the electric field, current and charge density read:

$$\begin{aligned} \mathbf{E} &= -\frac{1}{\gamma} \mathbf{u} \times \mathbf{B} = \frac{u_z B_y}{\gamma} \mathbf{e}_x - \frac{u_x B_y}{\gamma} \mathbf{e}_z, \\ \mathbf{j} &= \frac{c}{4\pi} \partial_x B_y \mathbf{e}_z, \\ \rho_{\text{pl}} &= -\rho_{\text{cr}} + \frac{1}{4\pi} \partial_x E_x. \end{aligned} \quad (\text{A1})$$

The four velocity of the inflowing plasma is written  $(\gamma c, \mathbf{u}c)$  (hence  $\mathbf{u} = \gamma \beta$  is dimensionless). In this equation,  $\gamma$  represents the total

Lorentz factor of the upstream plasma; it will be shown to coincide nearly with  $\Gamma_{\text{sh}}$  in the following.

Note that in the shock front, there is no current at zeroth order associated with the cosmic rays, only a net charge density  $\rho_{\text{cr}}$  which may be partially screened by an induced non-zero plasma charge density  $\rho_{\text{pl}}$ . Faraday's law implies in this stationary regime:

$$\nabla \times \mathbf{E} = 0 \leftrightarrow \partial_x \left( \frac{u_x B_y}{\gamma} \right) = 0, \quad (\text{A2})$$

Hence the Gauss equation can be rewritten as:

$$\rho_{\text{pl}} = -\rho_{\text{cr}} + \frac{B_y}{4\pi\gamma} \left( \partial_x u_z - \frac{u_z}{u_x} \partial_x u_x \right). \quad (\text{A3})$$

Energy momentum conservation for the upstream fluid implies:

$$\rho_u c^2 \mathbf{u} \cdot \nabla \mathbf{u} = \rho_{\text{pl}} \mathbf{E} + \frac{1}{c} \mathbf{j} \times \mathbf{B}, \quad (\text{A4})$$

where  $\rho_u$  is the proper mass density of the upstream plasma. Denoting  $F_m \equiv -\rho_u c^2 u_x$  the mass flux (times  $c$ ) through the shock front:

$$\begin{aligned} F_m \partial_x u_x &= \left[ \rho_{\text{cr}} - \frac{B_y}{4\pi\gamma} \left( \partial_x u_z - \frac{u_z}{u_x} \partial_x u_x \right) \right] \frac{u_z B_y}{\gamma} \\ &\quad + \frac{1}{4\pi} B_y \partial_x B_y, \\ F_m \partial_x u_z &= - \left[ \rho_{\text{cr}} - \frac{B_y}{4\pi\gamma} \left( \partial_x u_z - \frac{u_z}{u_x} \partial_x u_x \right) \right] \frac{u_x B_y}{\gamma}. \end{aligned} \quad (\text{A5})$$

Since:  $\gamma = (1 + u_x^2 + u_z^2)^{1/2}$ ,

$$\partial_x \gamma = \frac{u_x \partial_x u_x + u_z \partial_x u_z}{\gamma}, \quad (\text{A6})$$

therefore (A2) implies:

$$\partial_x B_y = -B_y \frac{\gamma}{u_x} \left( \frac{\gamma^2 - u_x^2}{\gamma^3} \partial_x u_x - \frac{u_x u_z}{\gamma^3} \partial_x u_z \right). \quad (\text{A7})$$

Using (A7), the system (A5) can be transformed into:

$$\begin{aligned} \left( F_m - \frac{B_y^2}{4\pi\gamma^2 u_x} \right) \partial_x u_x &= \rho_{\text{cr}} \frac{u_z B_y}{\gamma} \\ \frac{B_y^2 u_z}{4\pi\gamma^2} \partial_x u_x + \left( F_m - \frac{B_y^2 u_x}{4\pi\gamma^2} \right) \partial_x u_z &= -\rho_{\text{cr}} \frac{u_x B_y}{\gamma}. \end{aligned} \quad (\text{A8})$$

This system can be solved by successive approximations. For instance the ratio:

$$\left| \frac{B_y^2}{4\pi\gamma^2 u_x F_m} \right| \sim \frac{1}{\Gamma_{\text{sh}}^2} \beta_A^2 \ll 1 \quad (\text{A9})$$

since  $|u_x| \sim \Gamma_{\text{sh}}$ ;  $\beta_A = B_y / \sqrt{4\pi\rho_u c^2}$  represents the Alfvén velocity (as measured in the upstream rest frame). Hence:

$$\partial_x u_x \simeq \rho_{\text{cr}} \frac{u_z B_y}{\gamma F_m}. \quad (\text{A10})$$

Consider now the ratio of the first term on the lhs of the second equation in (A8) to the term of the rhs of the same equation:

$$\left| \frac{\partial_x u_x \frac{B_y^2 u_z}{4\pi\gamma^2}}{\rho_{\text{cr}} \frac{u_x B_y}{\gamma}} \right| \sim \frac{u_z^2}{\Gamma_{\text{sh}}^2} \beta_A^2. \quad (\text{A11})$$



This ratio is much smaller than unity (since  $u_z \ll \Gamma_{\text{sh}}$ ). Then:

$$\begin{aligned} \partial_x u_z &\simeq \rho_{\text{cr}} \frac{B_y}{F_m + \frac{B_y^2}{4\pi\gamma}} \\ \Rightarrow u_z(x) &\simeq \frac{B_y}{F_m + \frac{B_y^2}{4\pi\Gamma_{\text{sh}}}} \int_{x^*}^x \rho_{\text{cr}} dx. \end{aligned} \quad (\text{A12})$$

In the last equation,  $x_*$  corresponds to the maximal distance to which cosmic rays can stream ahead of the shock front, as measured in the shock front frame. We also assume that  $u_x$ ,  $B_y$  and  $\rho$  vary on much longer scales than  $u_z$ , and that  $|u_z| \ll |u_x|$ . This hierarchy can be verified by taking the ratios of the equations in (A5).

Since  $B_y^2/(4\pi\gamma) \approx \beta_A^2 F_m$ , one can simplify the previous expression and obtain the following order of magnitude:

$$|u_z| \sim \frac{\ell_{\text{cr}}}{r_{L*}} \frac{e_{\text{cr}}}{\Gamma_{\text{sh}} \rho_u c^2}. \quad (\text{A13})$$

To obtain this result, we have approximated the integral over  $\rho_{\text{cr}}$  as  $\ell_{\text{cr}} \rho_{\text{cr}}$ ,  $\ell_{\text{cr}}$  representing the length scale of the distribution in the shock frame, and written  $\rho_{\text{cr}} \simeq e_{\text{cr}}/(p_* c)$ ;  $e_{\text{cr}}$  denotes the cosmic ray energy density while  $p_*$  ( $r_{L*}$ ) represents their typical momentum (Larmor radius). Finally,  $e_{\text{cr}}/(\Gamma_{\text{sh}} \rho_u c^2) \sim \Gamma_{\text{sh}} \xi_{\text{cr}}$  where  $\xi_{\text{cr}}$  is the fraction of shock internal energy carried away by the accelerated population. In a straightforward way, one obtains:

$$\frac{\ell_{\text{cr}}}{r_{L*}} \sim \mathcal{O}(1), \quad (\text{A14})$$

so that:

$$\frac{|u_z|}{|u_x|} \sim \xi_{\text{cr}} \ll 1. \quad (\text{A15})$$

This justifies the previous approximations.

## A2 Time dependent quantities

### A2.1 Perturbed electric field

The perturbed Ohm law leads to:

$$\begin{aligned} \delta \mathbf{E} &= \frac{1}{\gamma} \left[ B_y \delta u_z + u_z \delta B_y + \right. \\ &\quad \left. + \frac{1}{\gamma^2} \left( \Gamma_{\text{sh}} \beta_{\text{sh}} u_z \delta u_x B_y - \delta u_x u_z^2 B_y \right) \right] \mathbf{e}_x + \\ &\quad \frac{1}{\gamma} \left( -\delta B_x u_z + \delta B_z u_x \right) \mathbf{e}_y + \\ &\quad \frac{1}{\gamma} \left[ \Gamma_{\text{sh}} \beta_{\text{sh}} \delta B_y - \delta u_x B_y + \right. \\ &\quad \left. + \frac{1}{\gamma^2} \left( \Gamma_{\text{sh}}^2 \beta_{\text{sh}}^2 \delta u_x B_y - \Gamma_{\text{sh}} \beta_{\text{sh}} \delta u_z u_z B_y \right) \right] \mathbf{e}_z. \end{aligned} \quad (\text{A16})$$

We keep track of the terms in  $u_z$  in these equations in order to properly evaluate the terms which involve the derivative of  $u_z$  with respect to  $x$ . This latter quantity is of the same order than other background quantities and cannot be neglected. However, terms in  $u_z$  will be neglected in the final equations of evolution of the various background quantities since  $u_z \ll u_x$ . For similar reasons, derivatives of background quantities (other than  $u_z$ ) such as  $\rho_{\text{pl}}$ ,  $B_y$  and  $u_x$  (hence  $\gamma$ ) can be neglected. Thus, setting  $\gamma \approx \Gamma_{\text{sh}}$ ,  $\beta \approx \beta_{\text{sh}}$  we

obtain:

$$\begin{aligned} \delta \mathbf{E} &= \left( \frac{1}{\Gamma_{\text{sh}}} B_y \delta u_z + \frac{1}{\Gamma_{\text{sh}}} u_z \delta B_y + \frac{\beta_{\text{sh}}}{\Gamma_{\text{sh}}^2} u_z B_y \delta u_x \right. \\ &\quad \left. + -\frac{1}{\Gamma_{\text{sh}}^3} u_z^2 B_y \delta u_z \right) \mathbf{e}_x + \\ &\quad \left( -\beta_{\text{sh}} \delta B_z - \frac{1}{\Gamma_{\text{sh}}} \delta B_x u_z \right) \mathbf{e}_y + \\ &\quad \left( \beta_{\text{sh}} \delta B_y - \frac{1}{\Gamma_{\text{sh}}} B_y \beta_{\text{sh}} \delta u_z u_z - \frac{1}{\Gamma_{\text{sh}}^3} B_y \delta u_x \right) \mathbf{e}_z. \end{aligned} \quad (\text{A17})$$

### A2.2 Perturbed equations

The perturbed equations for the perturbed components of the magnetic field, defined in units of  $B_y$ , as  $\mathbf{b} = \delta \mathbf{B}/B_y$  can be written:

$$\begin{aligned} \hat{D} b_x &= \frac{1}{\Gamma_{\text{sh}}^2} \partial_y \delta u_x + u_z \left( -\partial_z b_x + \frac{\beta_{\text{sh}}}{\Gamma_{\text{sh}}} \partial_y \delta u_z \right), \\ \hat{D} b_y &= -\partial_z \delta u_z - \frac{1}{\Gamma_{\text{sh}}^2} \partial_x \delta u_x - \frac{\beta_{\text{sh}}}{\Gamma_{\text{sh}}} u'_z \delta u_z + \\ &\quad + u_z \left( -\partial_z b_y - \frac{\beta_{\text{sh}}}{\Gamma_{\text{sh}}} \partial_z \delta u_x - \frac{\beta_{\text{sh}}}{\Gamma_{\text{sh}}} \partial_x \delta u_z + \right. \\ &\quad \left. + \frac{1}{\Gamma_{\text{sh}}^2} u_z \partial_z \delta u_z \right), \\ \hat{D} b_z &= \partial_y \delta u_z + u'_z b_x + u_z \left( \partial_x b_x + \partial_y b_y + \frac{\beta_{\text{sh}}}{\Gamma_{\text{sh}}} \partial_y \delta u_x + \right. \\ &\quad \left. - \frac{u_z}{\Gamma_{\text{sh}}^2} \partial_y \delta u_z \right). \end{aligned} \quad (\text{A18})$$

The continuity equation can be expressed as:

$$\hat{D} \frac{\delta w}{w} = -\nabla \cdot \delta \mathbf{u} - \frac{1}{c} \partial_t \delta \gamma \simeq -(\partial_x \delta u_x + \partial_y \delta u_y + \partial_z \delta u_z). \quad (\text{A19})$$

We have noted  $w = \rho_u c^2$  the proper enthalpy density of the upstream plasma. In the perturbation regime the contribution of the temporal derivative of the fluctuating part of the Lorentz factor is negligible. Again, while deriving Eq.(A19) the  $x$  derivatives of zeroth order quantities have been discarded.

The equation of motion in the shock rest frame accounting for the displacement current are:

$$w \hat{D} \mathbf{u} = \rho_{\text{pl}} \mathbf{E} - \nabla \frac{B^2}{8\pi} + \mathbf{B} \cdot \nabla \frac{\mathbf{B}}{4\pi} - \frac{1}{4\pi c} \frac{\partial \mathbf{E}}{\partial t} \times \mathbf{B}. \quad (\text{A20})$$

Using Eq.(A17) and developing the Eq.(A20) to the first order we

finally get after some manipulations:

$$\begin{aligned}
 \hat{D}\delta u_x &= \beta_A^2 \Gamma_{\text{sh}}^2 (\partial_y b_x - \partial_x b_y) - \kappa \delta u_z + \\
 &+ \beta_A^2 \Gamma_{\text{sh}}^2 \left( \beta_{\text{sh}} \frac{1}{c} \partial_t b_y - \frac{1}{\Gamma_{\text{sh}}^3 c} \partial_t \delta u_x \right) - \beta_s^2 \partial_x \frac{\delta w}{w} + \\
 &+ u_z \left[ \kappa (\beta_A^2 - 1) b_y + \frac{\beta_{\text{sh}}}{\Gamma_{\text{sh}}} \kappa (\beta_A^2 - 1) \delta u_x + \right. \\
 &+ \beta_{\text{sh}} \Gamma_{\text{sh}} \beta_A^2 (\partial_z b_y - \partial_y b_z) + \\
 &+ (\beta_{\text{sh}}^2 \beta_A^2 - \beta_A^2 - 1) \partial_z \delta u_x + \\
 &+ \left. \beta_A^2 \left( \partial_x \delta u_z - \beta_{\text{sh}} \frac{1}{c} \partial_t \delta u_z \right) \right], \\
 \hat{D}\delta u_y &= \beta_{\text{sh}} \Gamma_{\text{sh}} \kappa b_z - \beta_s^2 \partial_y \frac{\delta w}{w} + u_z (\kappa b_x - \partial_z \delta u_y), \\
 (1 + \beta_A^2) \hat{D}\delta u_z &= \beta_A^2 (\partial_y b_z - \partial_z b_y) - \beta_{\text{sh}} \Gamma_{\text{sh}} \kappa (1 - \beta_A^2) b_y + \\
 &- \kappa \beta_{\text{sh}}^2 (1 - \beta_A^2) \delta u_x - \frac{\beta_{\text{sh}}}{\Gamma_{\text{sh}}} \beta_A^2 \partial_z \delta u_x + \\
 &- \beta_s^2 \partial_z \frac{\delta w}{w} + \beta_{\text{sh}} \Gamma_{\text{sh}} \kappa \frac{\delta w}{w} + \\
 &+ u_z \left[ \frac{\beta_{\text{sh}}}{\Gamma_{\text{sh}}} (1 - 2\beta_A^2) \kappa \delta u_z - (1 + \beta_{\text{sh}}^2 \beta_A^2) \partial_z \delta u_z + \right. \\
 &+ \beta_{\text{sh}} \Gamma_{\text{sh}} \beta_A^2 (\partial_y b_x - \partial_x b_y) + \\
 &+ \beta_{\text{sh}} \beta_A^2 \left( \frac{1}{c} \partial_t \delta u_x - \beta_{\text{sh}} \partial_x \delta u_x \right) + \\
 &+ \left. \beta_A^2 \Gamma_{\text{sh}} \left( \frac{1}{c} \partial_t b_y - \beta_{\text{sh}} \partial_x b_y \right) \right]. \quad (\text{A21})
 \end{aligned}$$

We used the shorthand notation  $\beta_s^2 = c_s^2/c^2$  with  $c_s$  the speed of sound, and:

$$\beta_A^2 \equiv \frac{B_y^2}{4\pi \Gamma_{\text{sh}}^2 w}, \quad (\text{A22})$$

which defines the Alfvén velocity squared (as measured upstream). The quantity  $\kappa$ , which carries the dimension of a wavenumber, is defined as follows:

$$\kappa \equiv u'_z = \frac{1}{1 + \beta_A^2} \frac{\rho_{\text{cr}} B_y}{\Gamma_{\text{sh}} w}. \quad (\text{A23})$$

The plasma charge density  $\rho_{\text{pl}}$  is indeed related to the cosmic-ray charge density  $\rho_{\text{cr}}$  through the Maxwell equation:

$$\rho_{\text{pl}} = -\rho_{\text{cr}} + \frac{B_y}{4\pi \Gamma_{\text{sh}}} u'_z, \quad (\text{A24})$$

hence:

$$\frac{\rho_{\text{pl}} B_y}{\Gamma_{\text{sh}} w} = -\kappa. \quad (\text{A25})$$

In the limit  $\beta_A \ll 1$  and  $\beta_s \ll 1$ , the system governing the

evolution of the perturbed quantities reads:

$$\begin{aligned}
 \hat{D}b_x &= \frac{1}{\Gamma_{\text{sh}}^2} \partial_y \delta u_x + u_z \left( -\partial_z b_x + \frac{\beta_{\text{sh}}}{\Gamma_{\text{sh}}} \partial_y \delta u_z \right), \\
 \hat{D}b_y &= -\partial_z \delta u_z - \frac{1}{\Gamma_{\text{sh}}^2} \partial_x \delta u_x - \frac{\beta_{\text{sh}}}{\Gamma_{\text{sh}}} \kappa \delta u_z + \\
 &+ u_z \left( -\partial_z b_y - \frac{\beta_{\text{sh}}}{\Gamma_{\text{sh}}} \partial_z \delta u_x - \frac{\beta_{\text{sh}}}{\Gamma_{\text{sh}}} \partial_x \delta u_z \right), \\
 \hat{D}b_z &= \partial_y \delta u_z + \kappa b_x + u_z \left( -\partial_z b_z + \frac{\beta_{\text{sh}}}{\Gamma_{\text{sh}}} \partial_y \delta u_x \right), \\
 \hat{D}\delta u_x &= -\kappa \delta u_z - u_z \left( \kappa b_y + \beta_{\text{sh}} \frac{\kappa}{\Gamma_{\text{sh}}} \delta u_x + \partial_z \delta u_x \right), \\
 \hat{D}\delta u_y &= \beta_{\text{sh}} \Gamma_{\text{sh}} \kappa b_z + u_z (\kappa b_x - \partial_z \delta u_y), \\
 \hat{D}\delta u_z &= -\beta_{\text{sh}} \Gamma_{\text{sh}} \kappa b_y + \frac{\kappa}{\Gamma_{\text{sh}}^2} \delta u_x + \beta_{\text{sh}} \Gamma_{\text{sh}} \kappa \frac{\delta w}{w} + u_z \left( \frac{\beta_{\text{sh}}}{\Gamma_{\text{sh}}} \kappa \delta u_z - \partial_z \delta u_z \right), \\
 \hat{D}\frac{\delta w}{w} &= -\partial_x \delta u_x - \partial_y \delta u_y - \partial_z \delta u_z. \quad (\text{A26})
 \end{aligned}$$

To analyze the instabilities, it is convenient to make the following reduction:  $\hat{D} = k_x \beta_{\text{sh}} \Gamma_{\text{sh}} \tilde{D}$ ,  $\delta u_j = \beta_{\text{sh}} \Gamma_{\text{sh}} \tilde{u}_j$ ;  $b_j$  and  $\frac{\delta w}{w}$  unchanged. The ordering for doing simplifications is consistent with the expected physics: we assume  $k_y, k_z, k_* \ll k_x$ ,  $u_z \ll \beta_{\text{sh}} \Gamma_{\text{sh}}$  and  $\tilde{D}u_z = -\Gamma_{\text{sh}} k_* / k_x$  at the same order than previous terms. The simplified system reads:

$$\tilde{D}b_x \approx 0 \quad (\text{A27})$$

$$\tilde{D}b_y \approx -\frac{\partial_z}{k_x} \tilde{u}_z - \beta_{\text{sh}} \frac{k_*}{k_x} \tilde{u}_z - \beta_{\text{sh}}^2 \frac{u_z}{\beta_{\text{sh}} \Gamma_{\text{sh}}} \frac{\partial_x}{k_x} \tilde{u}_z \quad (\text{A28})$$

$$\tilde{D}b_z \approx \frac{\partial_y}{k_x} \tilde{u}_z \quad (\text{A29})$$

$$\tilde{D}\tilde{u}_x \approx -\frac{1}{\beta_{\text{sh}}} \frac{k_*}{k_x} \tilde{u}_z \quad (\text{A30})$$

$$\tilde{D}\tilde{u}_y \approx \frac{1}{\beta_{\text{sh}}} \frac{k_*}{k_x} b_z \quad (\text{A31})$$

$$\tilde{D}\tilde{u}_z \approx -\frac{1}{\beta_{\text{sh}}} \frac{k_*}{k_x} b_y + \frac{1}{\beta_{\text{sh}}} \frac{k_*}{k_x} \frac{\delta w}{w} \quad (\text{A32})$$

$$\tilde{D}\frac{\delta w}{w} \approx -\left( \frac{\partial_x}{k_x} \tilde{u}_x + \frac{\partial_y}{k_x} \tilde{u}_y + \frac{\partial_z}{k_x} \tilde{u}_z \right) \quad (\text{A33})$$

Thus one gets the intermediate system:

$$\begin{aligned}
 \tilde{D}^2 \tilde{u}_z &= \left( \frac{k_*^2}{k_x^2} + \frac{k_* \partial_z}{\beta_{\text{sh}} k_x^2} + \beta_{\text{sh}} \frac{u_z}{u_{\text{sh}}} \frac{k_* \partial_x}{k_x} \right) \tilde{u}_z + \frac{k_*}{\beta_{\text{sh}} k_x} \tilde{D} \frac{\delta w}{w} \\
 \tilde{D}^3 \frac{\delta w}{w} &= \frac{k_* \partial_x}{\beta_{\text{sh}} k_x^2} \tilde{D} \tilde{u}_z - \frac{k_* \partial_y^2}{\beta_{\text{sh}} k_x^3} \tilde{u}_z - \frac{\partial_z}{k_x} \tilde{D}^2 \tilde{u}_z \quad (\text{A34})
 \end{aligned}$$

## REFERENCES

- Achterberg, A., Gallant, Y., Kirk, J. G., Guthmann, A. W., 2001, *MNRAS* 328, 393  
 Amato, E., & Blasi, P. 2008, arXiv:0806.1223  
 Bell, A., 2004, *MNRAS*, 353, 550  
 Bell, A., 2005, *MNRAS*, 358, 181  
 Blandford, R., McKee, C., 1976, *Phys. Fluids*, 19, 1130  
 Chang, P., Spitkovsky, A., & Arons, J. 2008, *ApJ*, 674, 378  
 Dieckmann, M. E., Shukla, P. K., Drury, L. O. C., 2008, *ApJ*, 675, 586.  
 Frederiksen, J. T., Hededal, C. B., Haugbølle, T., & Nordlund, Å. 2004, *ApJ*, 608, L13  
 Gallant, Y., Achterberg, A., 1999, *MNRAS* 305, L6  
 Genet, F., Daigne, F., Mochkovitch, R., 2007, *MNRAS* 381, 732

- Gruzinov, A., Waxman, E., 1999, ApJ, 511, 852  
Hededal, C. B., Nishikawa, K. I., 2005, ApJ, 623, L89  
Hoshino, M., 2008, ApJ, 672, 940  
Kato, T. N., 2007, ApJ, 668, 974  
Katz, J. I., 1994, ApJ, 432, L107  
Keshet, U., Katz, B., Spitkovsky, A., Waxman E., 2008, arXiv:0802.3217  
Lemoine, M., Pelletier, G., 2003, ApJ, 589, L73  
Lemoine, M., Revenu, B., 2006, MNRAS 366, 635  
Lemoine, M., Pelletier, G., Revenu, B., 2006, ApJ, 645, L129  
Li, Z., Waxman, E., 2006, ApJ, 651, L328  
Lyubarsky, Y., Eichler, D., 2006, ApJ, 647, L1250  
Marcowith, A., Lemoine, M., Pelletier, G., 2006, AA, 453, 193  
Medvedev, M. V., Loeb, A., 1999, ApJ, 526, 697  
Medvedev, M. V., Fiore, M., Fonseca, R. A., Silva, L. O., & Mori, W. B. 2005, ApJ, 618, L75  
Milosavljević, M., Nakar, E., 2006, ApJ, 651, 979  
Niemiec, J., Ostrowski, 2006, ApJ, 641, 984  
Niemiec, J., Ostrowski, M., Pohl, M., 2006, ApJ, 650, 1020  
Niemiec, J., Pohl, M., Stroman, T., & Nishikawa, K. I. 2008, ApJ, 684, 1174  
Mészáros, P., Rees, M., 1997, ApJ, 476, 232  
Parizot, E., Marcowith, A., Ballet, J. & Gallant, Y.A., 2006, A&A, 453, 387  
Paczyński, B., Rhoads, J. E., 1993, ApJ 418, L5  
Pelletier, G., Lemoine, M., Marcowith, A., 2006, AA, 453, 181  
Piran, T., 2005, Rev. Mod. Phys., 76, 1143  
Reville, B., Kirk, J. G., Duffy, P., 2006, Plasma Phys. Contr. Fus., 48, 1741  
Reville, B., Kirk, J. G., Duffy, P., O'Sullivan, S., 2007, AA, 475, 435  
Reville, B., O'Sullivan, S., Duffy, P., Kirk, J. G., 2008, MNRAS, 386, 509  
Sari, R., Piran, T. 1997, ApJ, 485, 270  
Silva, L. O., Fonseca, R. A., Tonge, J. W., Dawson, J. M., Mori, W. B., & Medvedev, M. V. 2003, ApJ, 596, L121  
Spitkovsky, A., 2008, arXiv:0802.3216  
Uhm, Z. L., Beloborodov, A. M., 2006, ApJ 665, L93  
Vietri, M. 1997, ApJ, 478, L9  
Völk, H.J., Berezhko, E.G. & Ksenofontov, L.T., 2005, A&A, 433, 229  
Waxman, E., 1997, ApJ 485, L5  
Wiersma, J., Achterberg, A., 2004, AA, 428, 365  
Zirakashvili, V. N., Ptuskin, V. S., & Völk, H. J. 2008, ApJ, 678, 255